Hindawi
Journal of Nanomaterials
Volume 2018, Article ID 5268458, 9 pages
https://doi.org/10.1155/2018/5268458

Research Article

SPR-Enhanced Fluorescence of Solid Organic Dye Films

Qing Fu,[1] Xiaolin Zhang,[1] Peipei Yan,[1] Shichao Wang,[1] Xinzhi Wang,[1] Yao Wang,[1] Linjun Huang,[1] Yanxin Wang,[1] Haiyan Liu,[1] Laurence A. Belfiore,[2] and Jianguo Tang[1]

[1]*Institute of Hybrid Materials, National Center of International Research for Hybrid Materials Technology, National Base of International Science & Technology Cooperation, College of Materials Science and Engineering, Qingdao University, Qingdao 266071, China*
[2]*Department of Chemical and Biological Engineering, Colorado State University, Fort Collins, CO 80523, USA*

Correspondence should be addressed to Laurence A. Belfiore; belfiore@colostate.edu and Jianguo Tang; tang@qdu.edu.cn

Received 6 February 2018; Revised 18 April 2018; Accepted 15 May 2018; Published 23 August 2018

Academic Editor: Mohamed Bououdina

This paper presents strong fluorescence of spin-coated fluorescent solid organic dye films (SODF) enhanced by surface plasmonic resonance (SPR). In order to manifest the influence of SPR effect on enhancement of organic dye (OD) fluorescence, the organic dye embedded Ag@SiO_2 fluorescent films were developed on the glass sheet substrate, in which Ag@SiO_2 nanoparticles were embedded in the middle and organic dye was as upper layer. The morphology of the SODFs with and without Ag@SiO_2 particles was studied by SEM and EDX, and the tests revealed that the Ag@SiO_2 nanoparticles distributed evenly between glass sheet and OD layer. Optical properties were characterized by UV absorption and fluorescence spectroscopy; the lifetime of SODF was tested to discuss the mechanism of SPR enhancement of fluorescence. The results proved that the existence of Ag@SiO_2 particles enhanced the fluorescence intensity for 7 times and thus proved the SPR effect for organic dye, especially when the organic dye is the solid films. Therefore, the most important is the creation that the SPR effect of Ag@SiO_2 particles works very well under solid organic dye coverage.

1. Introduction

In recent decades, organic fluorescent dyes have been widely used in many fields due to their superior properties including good optical property like high luminescence efficiency, rich variety of derivatives and relatively complete spectrum [1]. Among all the fluorescent dyes, rhodamine with a higher fluorescence quantum yield was widely used in biological dyes, fluorescent labels, and laser fuels. Dye molecules tend to associate driven by the synergistic effect (such as van der Waals forces, hydrogen bonding, charge interactions, and hydrophobic interactions) to form a dimer, trimer, or even multimer with supramolecular structure. Under the influence of different inducing forces, the aggregates formed by the dye molecules or ions can exhibit different arrangement forms and micromorphologies, thereby giving the dye special photophysical and photochemical properties [2–4]. But the good optical properties of rhodamine only appear in dilute solvents, when it is in high concentration or solid state, fluorescence quenching occurs because of the aggregate of rhodamine molecules. This phenomenon not only appeared in rhodamine but also in other fluorescent dyes. Therefore, it is a challenge to prepare solid fluorescent films which are required in the field of fundamental research and indication application [5–13].

Some groups tried to overcome the problems of organic dye luminescence weakness and photo stability limitations by using surface plasmon resonances (SPR) [1, 4, 14, 15]. To do that, nanosilver was used to enhance the fluorescent intensity in this study. SPR was performed by combining the amplification of the incident electric field at or near the surface of nanoparticles and the coupling of excited organic dyes (ODs) with the electrons in the particles [14, 15]. It can increase the fluorescence intensity of the organic dye, reduce its fluorescence lifetime, and improve the photochemical stability at the same time [16–18]. Maintaining

a certain space and structure between Ag particles and dye molecules has a positive effect on SPR [19], by designing a rational model. SPR can be a powerful means to enhance the optical properties of commercially available luminescent dyes [14, 20].

In our group, triple layer core-shell nanostructure of $Ag@SiO_2@Eu^{3+}$ complexes had developed, by using $Ag@SiO_2$ nanostructure to enhance the fluorescence of Eu^{3+} complexes, and the fluorescent intensity enhanced to 13 times comparing with Eu^{3+} complexes without $Ag@SiO_2$ [21]. However, the investigations have the prerequisite, that is, the samples that enhanced fluorescence are in liquid media. Based on this background, strong fluorescence of spin-coated SODFs enhanced by SPR are designed in this article. To give a comprehensive study on the $Ag@SiO_2$ under the solid organic dye films, three different organic dyes: rhodamine B (RB), fluorescein (FLU), and eosin Y (EY) were used. The morphology and distribution of $Ag@SiO_2$ under SODF were investigated using TEM and SEM. With the optimized $Ag@SiO_2$ distribution and concentration under spin-coated SODF, the fluorescent intensity has enhanced by 7 times comparing with non-SPR-enhanced SODF. With this breakthrough of SPR-enhanced SODFs, it can be applied in practical utilization like transportation safety and security, optoelectronic devices, energy transform in the films become possible.

2. Experimental Section

2.1. Materials. The chemicals used were silver nitrate (AR, Shanghai Pharmaceutical Group Co. Ltd.); sodium citrate (AR, Shanghai Hengda Fine Chemicals Co. Ltd.); glucose (AR, Sinopharm Chemical Reagent Co. Ltd.); sodium borohydride (Aladin Industrial Corporation); polyvinylpyrrolidone (PVP) (Mr = 24,000), rhodamine B (Analytical Pure, Aladdin Reagent Co. Ltd.); fluorescein (Adamas Reagent Co. Ltd); eosin Y (Aladin Industrial Corporation); concentrated ammonia (AR, Sinopharm Chemical Reagent Co. Ltd.); ethyl orthosilicate (AR, Sinopharm Chemical Reagent Co. Ltd.); ethanol (AR, Sinopharm Chemical Reagent Co. Ltd.); thickening agent (lab make); and some other common solvents. All the purchased chemicals were used as received without further purification.

2.2. Preparation of Silver and $Ag@SiO_2$ Nanoparticles. Silver nanoparticles were prepared according to the reported works [21, 22]. 0.159 g PVP, 0.051 g sodium citrate, 0.083 g glucose, and 30.184 g triple distilled water were added into a 100 ml three-necked flask; the mixture was stirred and refluxed at 103°C with an oil bath. 0.027 g silver nitrate and three drops of concentrated ammonia were added into 5 ml three distilled water. After the silver nitrate was completely dissolved, the solution was added dropwise into the flask for three times with an interval of 10 minutes. Finally, gray-green suspension was obtained.

7.2 ml above-prepared suspension, 2.7 ml concentrated ammonia, 80 ml ethanol, and 9.2 ml triple distilled water were added into a 150 ml single-necked flask and stirred under 40°C oil baths. 0.14 g of ethyl orthosilicate was added into 10 ml ethanol and stirred for a while until it dispersed evenly. After that, 1 ml of the solution was added into the single-necked flask drop in drop and stirred at a constant temperature for 2 hours. The precipitate collected using centrifugation was washed using ethanol to remove the unreacted reactants. The precipitate was dissolved in ethanol and stored in the refrigerator (usually valid for a week) [14, 22].

2.3. Formation of SODF. Firstly, the glass sheet was washed repeatedly using distilled water and ethanol, then ultrasonic for 10 min, and further washed using isopropanol before ultrasonic for another 10 min and dried under nitrogen atmosphere. Secondly, 20 ml clear homogeneous OD solutions (5×10^{-3} mol/L) were prepared by adding 1 g (5% weight to ethanol) thickening agent into RB, FLU, and EY ethanol solutions and stirring for more than 3 hours at room temperature. Finally, $Ag@SiO_2$ solution previously prepared was dropped onto the cleaned glass sheet and spin coated for 18 seconds at a rate of 300 r/min. After that, the OD solutions was dropped onto the silver layer and spin coated at a rate of 300 r/min for 18 s. SODF with $Ag@SiO_2$ ($Ag@SiO_2$@RB, $Ag@SiO_2$@FLU, and $Ag@SiO_2$@EY) were obtained.

2.4. Characterization. The morphology of dominating silver nanoparticles and $Ag@SiO_2$ was observed by transmission electron microscopy (TEM, 200 kv on a JEM-1200 EX, Japan). The distribution of $Ag@SiO_2$ and the coverage of dyes were characterized using scanning electron microscopy (SEM, JSM-7500F, JEOL Ltd.) and field emission scanning electron microscopy (JSM7610F; S4800); the thickness of the film can be measured by A3-ST Spectroscopic Transmission. The UV-Vis absorption spectra and fluorescence intensity spectral were obtained by UV/VIS/NIR Spectrometer (Lambda 750 S) and Fluorescence Spectrophotometer (Cary Eclipse, American Varian company), respectively. The lifetime was characterized by FLS980 Series of Fluorescence Spectrometer.

3. Results and Discussion

3.1. Characterization of Nanosilver Particles and $Ag@SiO_2$ Particles. The size and morphology of Ag particles and $Ag@SiO_2$ particles are showed in Figures 1(a) and 1(b), respectively. As is shown in Figure 1, $Ag@SiO_2$ particles were well prepared using Ag as the core with a size of 50 ± 10 nm and SiO_2 as the shell with a thickness of 25 ± 5 nm. Due to the fact that the size of Ag particles and SiO_2 shell thickness has great influence on the SPR-enhancement phenomenon. SPR enhancement fluorescence is relatively constant when the distance between Ag particles and dye molecules is greater than 5 nm [1, 16, 22–24]; the uniform SiO_2 shell can not only avoid the aggregate of Ag particles, it also gives a space to Ag and OD molecules. The size of Ag and $Ag@SiO_2$ particles used in the work was kept in the range showed in Figure 1 to avoid the influence of size on the SPR-enhanced fluorescence.

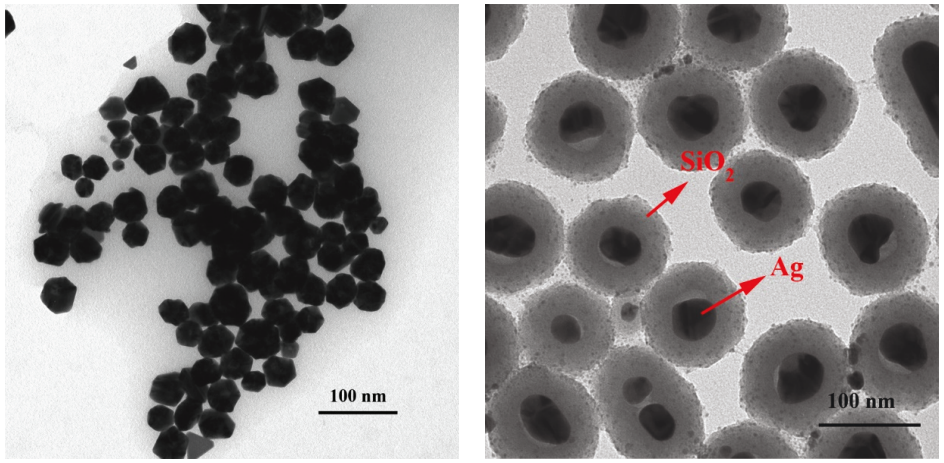

Figure 1: TEM images of Ag (a) and Ag@SiO_2 particles (b).

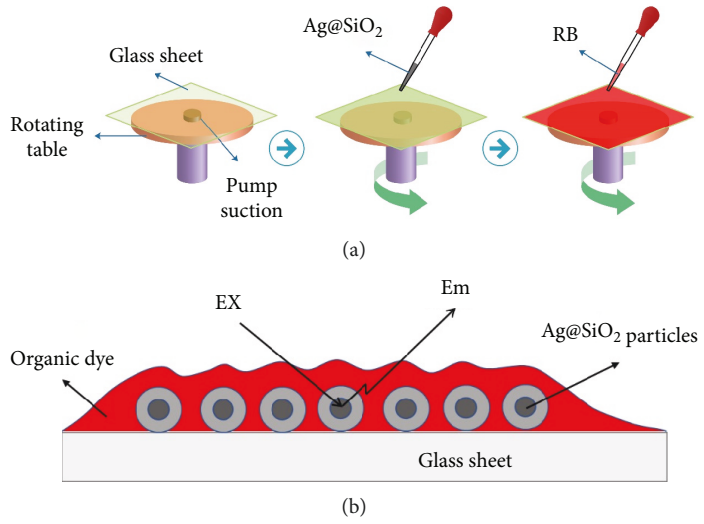

Figure 2: Schematic of spin-coated process (a) and SODF with Ag@SiO_2 structure (b).

3.2. Surface Morphology of Fluorescent Film. Figure 2(a) shows the preparation process of SODF with Ag@SiO_2; Ag@SiO_2 nanoparticles were spin coated on the glass sheet first and then coated a layer of organic dyes, thus formed the SODF (named Ag@SiO_2@OD), showed in Figure 2(b). Energy transfer in Ag@SiO_2@OD is simply presented in Figure 2(b). Here are two typical SPR mechanism models that can be found from the literatures, namely, radiative decay engineering (RDE) and surface plasmon-coupled emission. RDE model assumes that the presence of metal, the decay rate of the OD changes. When the excited OD returns to the ground state, the radiation decay rate increases. The fluorescent intensity of OD increased with the decay rate of radiation, while the lifetime of OD decreased. This surface-enhanced fluorescence can be obtained by controlling the rate of radiation decay [25–27]. Different with this model, surface plasmon-coupled emission model assumes that excited state of OD transfers energy in a nonradiative form to the plasma of metal surface, giving rise to fluorescence enhancement on the surface of metal. In this theoretical explanation, it is considered that excited-state fluorescent species and surface plasmon are the only radiation sources [28, 29]. Actually, the mechanism of SPR is very complicated. The two models were created to make it easier and faster to apply the theory to actual experimental studies; some related documents have explained this theory in detail [30–33].

In order to investigate the surface condition of SODF, the morphology of RB film and Ag@SiO_2@RB film was observed by SEM. From the experiment, we found that Ag particles are easily to aggregate and hard to spin coat on the glass sheet, because most Ag particles were throwed away by the centrifugal force during the process since large group of particles increased the probability of throwing away from the smooth glass surface. Figure S1a shows the SEM picture of Ag spin-coated film; the surface of the glass sheet was very clean

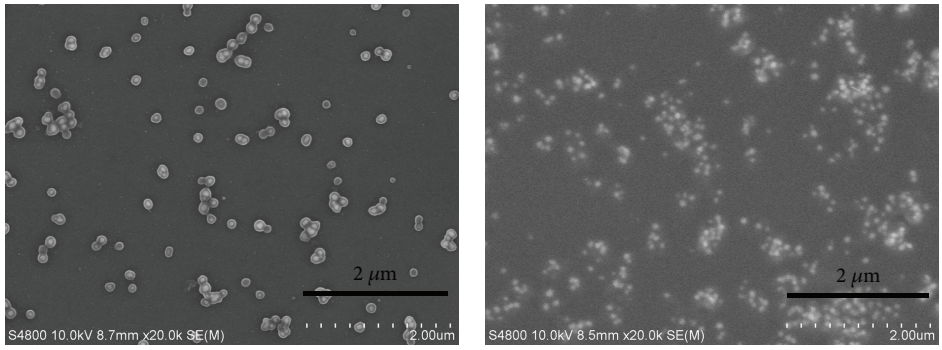

(a) (b)

Figure 3: SEM of $Ag@SiO_2$ and $Ag@SiO_2$@RB; (a) is Ag@SiO2 spin-coated on glass sheet and (b) is $Ag@SiO_2$@RB film.

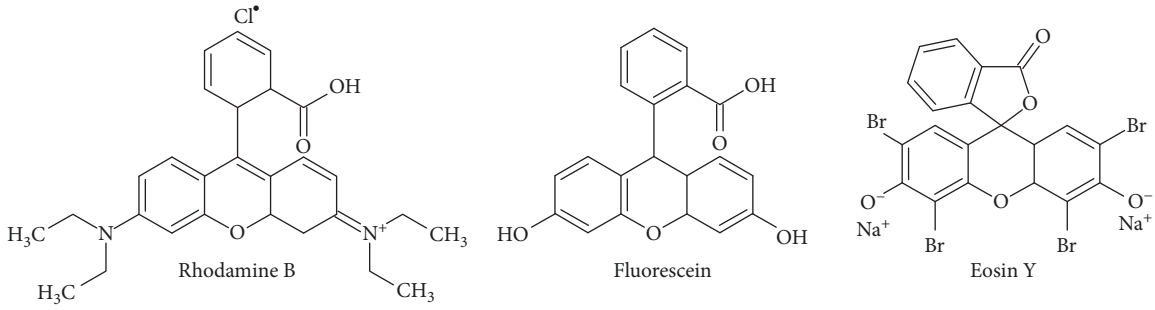

Figure 4: Chemical structures of different ODs: rhodamine B (RB), fluorescein (FLU), and eosin Y (EY).

and only a few Ag particles remained, while $Ag@SiO_2$ particles are observed to have well dispersed and attached on the glass sheet (Figure S1b). SiO_2 shell plays an important role in preventing the Ag particles to gather together and keeping a distance between Ag and OD molecules. Figure S1c is RB spin-coated film without other additions, and Figure S1d is the morphology of $Ag@SiO_2$@RB film. Due to the layer of RB, the dots in Figure S1d looked unclear and the size became smaller compared with Figure S1b. To further investigate the morphology of SODF film, field emission scanning electron microscopy (FESEM) and energy dispersive X-ray spectroscopy (EDX) were used to characterize the morphology and components. Figure 3 is the FESEM of $Ag@SiO_2$ and $Ag@SiO_2$@RB film, and EDX pictures of silver elements, nitrogen elements, and carbon elements distribution are given in supporting information (Figure S2).

The surface morphology of SODF looks relatively clear in Figure 3, especially the distribution of $Ag@SiO_2$ particles, which has a great influence on the optical properties in following tests. The morphology and distribution of $Ag@SiO_2$ particles were characterized in Figure 3(a), in general, the distribution of $Ag@SiO_2$ particles are relatively dense and uniform, the edge of $Ag@SiO_2$ particles are clear and independent. Figure 3(b) characterized the morphology of the $Ag@SiO_2$@RB film; the $Ag@SiO_2$ particles in the picture are vague and indistinct like hiding under something. That is to say, $Ag@SiO_2$ particles are embedded inside by the dye film, just as shown in Figure 2(b); the microscope disturbed by the organic materials on the surface of $Ag@SiO_2$ particles made it hard to focus on the particles, thus leading to the particle image blur.

3.3. Optical Properties of SODF. Three kinds of ODs were used in this work; the structures of these ODs were showed in Figure 4. The maximum absorption wavelength of RB, FLU, and EY was 560 nm [7, 34, 35], 525 nm [34, 36], and 540 nm [36, 37], respectively. The UV-Vis absorption spectrum of $Ag@SiO_2$ film was shown in Figure 5(a); the UV-Vis absorption spectra of RB, FLU, and EY SODF without and with $Ag@SiO_2$ are shown in Figures 5(b)–5(d), respectively. After the addition of $Ag@SiO_2$, all the SODF showed larger and wider absorption.

Fluorescence emission intensity of three kinds of SODF with and without $Ag@SiO_2$ particles is shown in Figure 6. Spectrogram (a) is RB film and $Ag@SiO_2$@RB film. The left one shows the maximum excitation wavelengths (λ_{ex}) of RB and $Ag@SiO_2$@RB film are different. Compared to RB film ($\lambda_{ex} = 565$ nm), peak of $Ag@SiO_2$@RB ($\lambda_{ex} = 562$ nm) has blue shift for 3 nm. This may be due to the effect of $Ag@SiO_2$ which has an absorption peak at 480 nm. When $Ag@SiO_2$ nanoparticles are near RB molecules, it may cause blue shift of RB excitation spectrogram. In order to contrast the emission intensity, we excited the films in 560 nm and got the right emission spectrogram; the λ_{em} of the films are both at 615 nm, but the emission intensity of $Ag@SiO_2$@RB film is higher than RB films which increase for about sevenfold. Spectrogram (b) is FLU and $Ag@SiO_2$@FLU film. The λ_{ex} of $Ag@SiO_2$@FLU has blue shift for 5 nm. We excited the

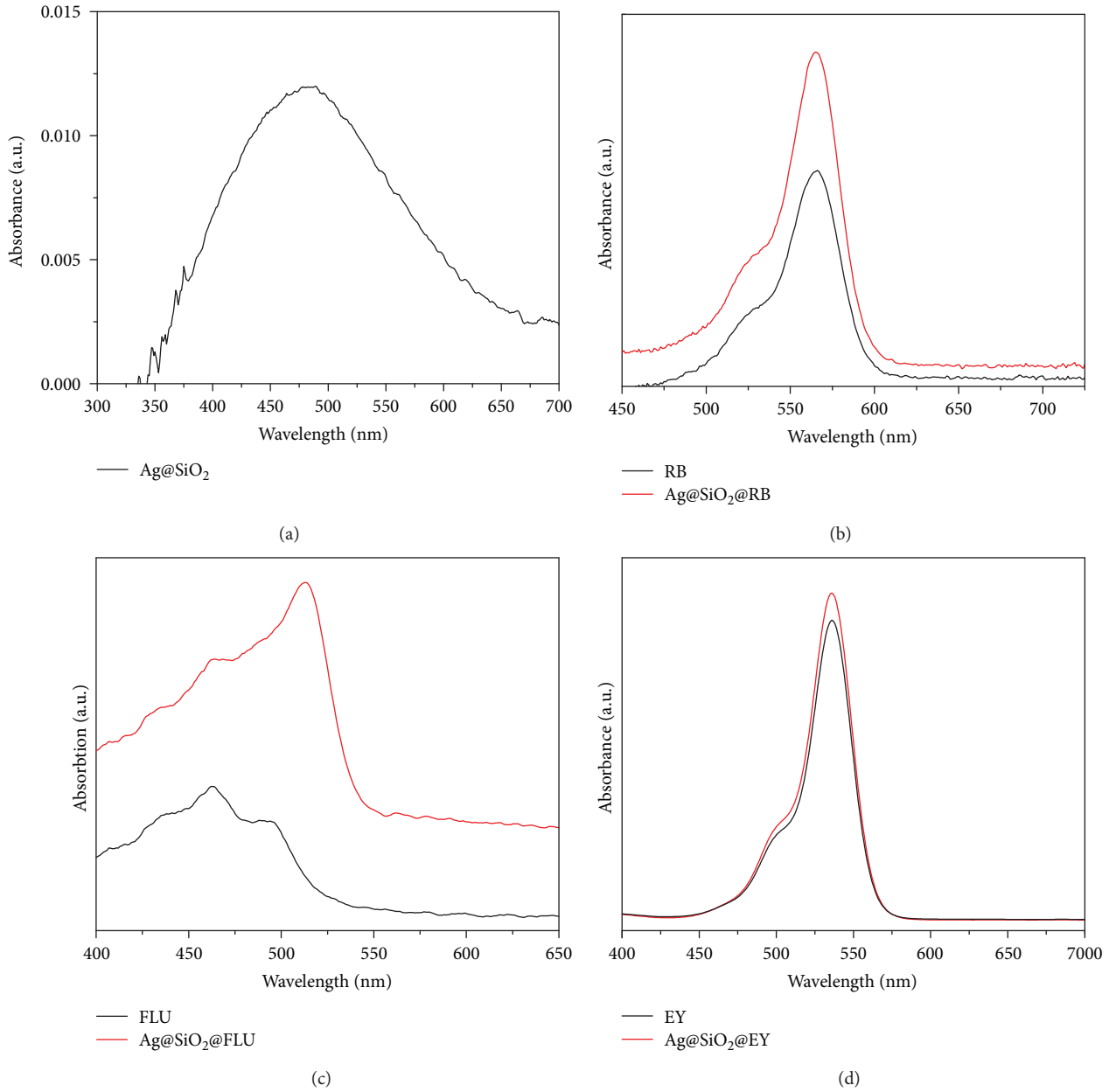

Figure 5: UV-Vis absorption spectra of SODF with and without $Ag@SiO_2$.

FLU films at 480 nm and got the emission spectrogram. The intensity of $Ag@SiO_2$@FLU film has increased for about 2.5-fold. Spectrogram (c) is EY and $Ag@SiO_2$@EY film. The λ_{ex} of $Ag@SiO_2$@EY film and EY film is almost the same. We excited the films at 545 nm and got the emission spectrogram. The emission intensity has increased for about twofold. The increase of fluorescence emission intensity owns to $Ag@SiO_2$ nanoparticles surface plasmon resonances to organic dyes.

Figure 7 is decay curves of fluorescence intensity with time. Here, we tested RB film and RB with $Ag@SiO_2$ film both excited in 560 nm. The average lifetime of RB film is 3.5034 ns and $Ag@SiO_2$@RB film is 2.9071 ns. Compared to Figures 6(a) and 7, the fluorescence intensity has increased to 7 times while the lifetime has decreased about 0.5 ns with the existence of $Ag@SiO_2$. Some reports have revealed that silver or gold nanoparticles can enhance fluorescence emission dramatically with the reduce of lifetime [38, 39]. There are several interactions between OD and $Ag@SiO_2$. Strong enhancement of fluorescence emission in this case may be due to two mechanisms: radiative decay engineering (RDE) [27] and surface plasmon-coupled emission [28]. The effect of RDE is a rapid release of the excitation energy and its radiation into free space; it results in an increase of fluorescent intensity and decrease of its lifetime [38]. Just as Figures 6(a) and 7 shows, $Ag@SiO_2$ nanoparticles SPR enhance RB film fluorescence intensity can be classified into this mechanism. It can also apply to the other two kinds of

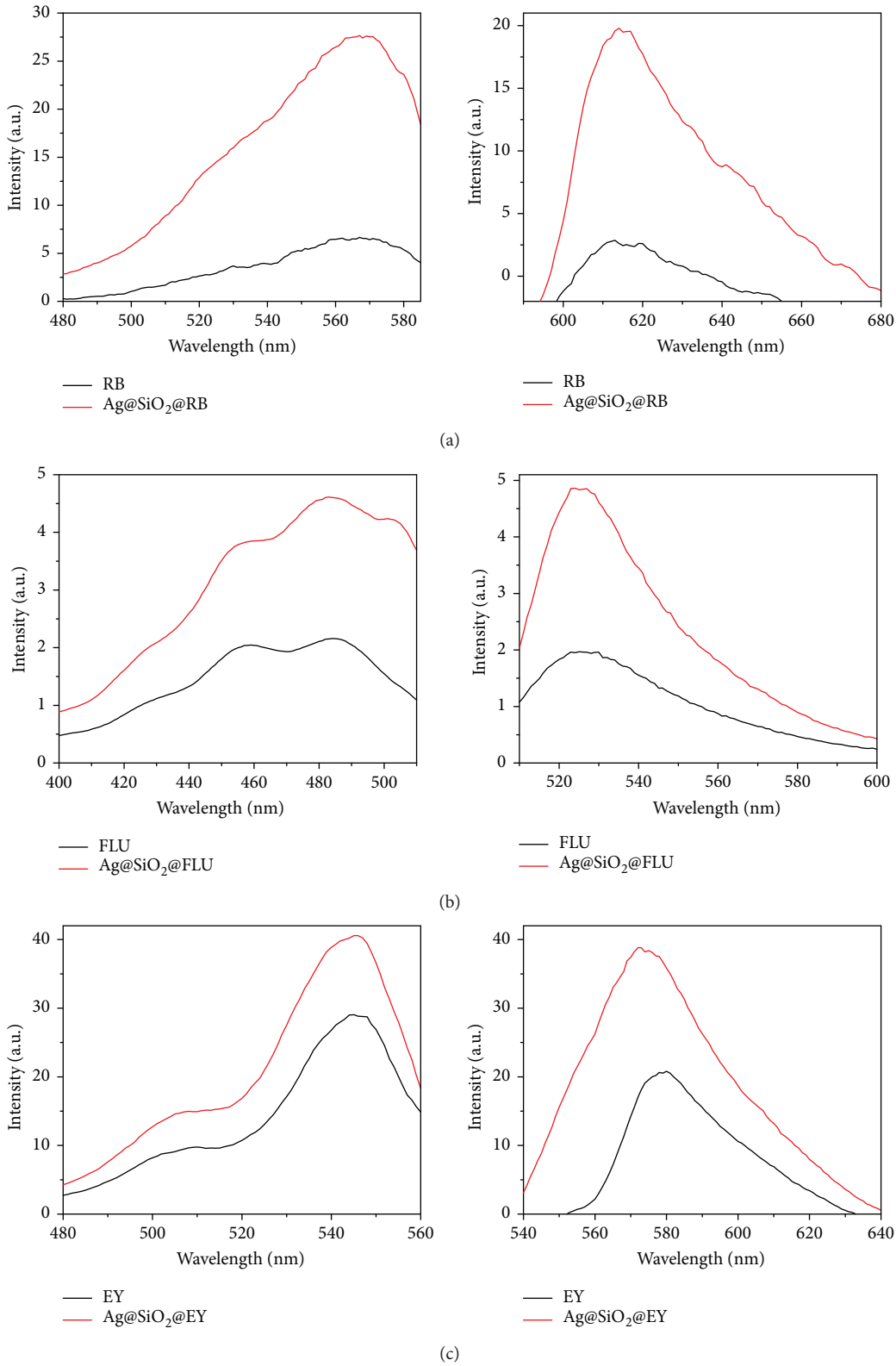

Figure 6: Fluorescence intensity for OD and Ag@SiO_2@OD. (a) Excitation (left) and emission (right) spectrogram of RB (film thickness: 92 ± 2 nm) and Ag@SiO_2@RB (film thickness: 90 ± 2 nm); emission spectrogram is got in $\lambda_{ex} = 560$ nm. (b) Excitation (left) and emission (right) spectrogram of FLU (film thickness: 68 ± 2 nm) and Ag@SiO_2@FLU (film thickness: 70 ± 2 nm); emission spectrogram is got in $\lambda_{ex} = 480$ nm. (c) Excitation (left) and emission (right) spectrogram of EY (film thickness: 105 ± 3 nm) and Ag@SiO_2@EY (film thickness: 103 ± 3 nm), emission spectrogram is got in $\lambda_{ex} = 545$ nm. All the spectrograms were got from 5 nm*5 nm excitation and emission slits.

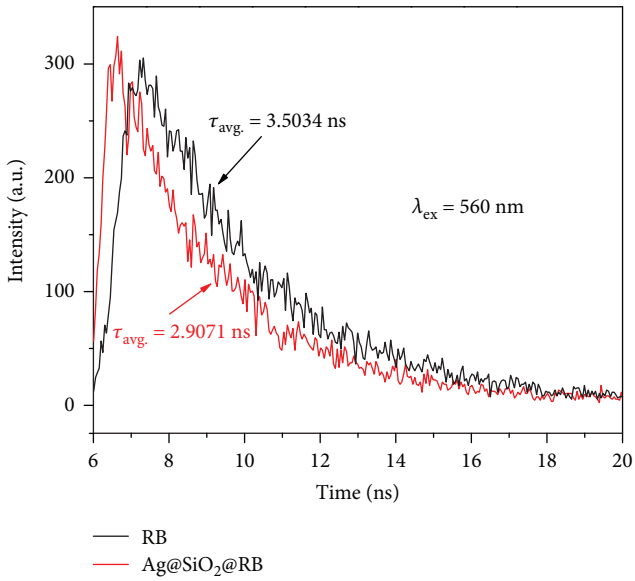

Figure 7: Fluorescence intensity decay curves of RB film and Ag@SiO_2@RB film.

Table 1: Average lifetime of OD films without and with Ag@SiO_2.

Samples (average lifetime/ns)	RB	FLU	EY
Without Ag@SiO_2	3.5034	4.6288	2.8106
With Ag@SiO_2	2.9071	4.3141	2.6452

dyes; the results have been listed in Table 1. The average lifetime of FLU and EY film have decreased with the effect of SPR. Fluorescence emission intensity of FLU increased for 2.5 times with the lifetime decreased for 0.3 ns, and EY fluorescence emission intensity increased for 2 times with the sacrifice of 0.2 ns lifetime.

It can be figured out that Ag@SiO_2 in SODF has a significant effect on fluorescence emission intensity; for different ODs, the affection is different. The mechanism of SPR is RDE theory; the OD fluorescence emission intensity increased with the sacrifice of lifetime. As previous studies have been shown [8–11], due to the solvent effect, OD in liquid state has high fluorescent property, whereas, in solid state, the concentration quenching effect greatly reduces the optical properties of fluorescent dyes. Therefore, the sevenfold fluorescence enhancement of Ag@SiO_2-in-SODF confirms the optimized structures are effective.

4. Conclusion

This paper mainly discussed SPR-enhanced fluorescence in SODF which were prepared by means of spin coating. The surface morphology and fluorescence properties of the films were investigated. SEM images showed that Ag@SiO_2 particles are embedded in the OD layer. The UV-Vis absorption spectra and fluorescence intensity spectra of SODF showed that the SODF with Ag@SiO_2 lead to an enhancement of intensity, with an enhancement of 2 to 7 times than SODF without Ag@SiO_2 particles. Based on the results, we demonstrated that the fluorescence intensity of SODF can be increased by the incorporation of Ag@SiO_2 thanks to the SPR effect.

Data Availability

The data used to support the findings of this study are available from the corresponding author upon request.

Conflicts of Interest

The authors declare that they have no conflicts of interest.

Acknowledgments

This work is supported by (1) the Natural Scientific Foundation of China (51473082, 51373081, and 51503112); (2) the National Program for Introducing Talents of Discipline to Universities ("111" plan); (3) the State Key Project of International Cooperation Research (2017YFE0108300, 2016YFE0110800); (4) The National One-Thousand Foreign Expert Program (Grant no. WQ20123700111); and (5) the Key Research and Development Plan of Shandong Province (Grant no. 2017 GGX20112).

Supplementary Materials

Figure S1: SEM images of spin-coated films ((a) Ag, (b) Ag@SiO2, (c) RB, (d) Ag@SiO2@RB). Figure S2: EDX of Ag@SiO2@RB film. (a) is the original SEM image, (b) is the distribution of silver element, (c) is the distribution of nitrogen element, and (d) is the distribution of carbon element. *(Supplementary Materials)*

References

[1] J. Asselin, P. Legros, A. Grégoire, and D. Boudreau, "Correlating metal-enhanced fluorescence and structural properties in Ag@SiO_2 core-shell nanoparticles," *Plasmonics*, vol. 11, no. 5, pp. 1369–1376, 2016.

[2] E. Donath, G. B. Sukhorukov, F. Caruso, S. A. Davis, and H. Möhwald, "Novel hollow polymer shells by colloid-templated assembly of polyelectrolytes," *Angewandte Chemie International Edition*, vol. 37, no. 16, pp. 2201–2205, 1998.

[3] P. Bojarski and A. Jankowicz, "Excitation energy transport between the ionic forms of rhodamine B in viscous solutions," *Journal of Luminescence*, vol. 81, no. 1, pp. 21–31, 1999.

[4] A. R. Guerrero and R. F. Aroca, "Surface-enhanced fluorescence with shell-isolated nanoparticles (SHINEF)," *Angewandte Chemie*, vol. 50, no. 3, pp. 665–668, 2011.

[5] D. Avnir, V. R. Kaufman, and R. Reisfeld, "Organic fluorescent dyes trapped in silica and silica-titania thin films by the sol-gel method. Photophysical, film and cage properties," *Journal of Non-Crystalline Solids*, vol. 74, no. 2-3, pp. 395–406, 1985.

[6] M. Uchida, Y. Ohmori, T. Noguchi, T. Ohnishi, and K. Yoshino, "Color-variable light-emitting diode utilizing conducting polymer containing fluorescent dye," *Japanese Journal of Applied Physics*, vol. 32, no. 7A, Part 2, pp. L921–L924, 1993.

[7] F. Lopezarbeloa, V. Martinezmartinez, T. Arbeloa, and I. Lopezarbeloa, "Photoresponse and anisotropy of rhodamine

dye intercalated in ordered clay layered films," *Journal of Photochemistry and Photobiology C Photochemistry Reviews*, vol. 8, no. 2, pp. 85–108, 2007.

[8] I. L. Arbeloa and P. R. Ojeda, "Dimeric states of rhodamine B," *Chemical Physics Letters*, vol. 87, no. 6, pp. 556–560, 1982.

[9] M. C. Gutiérrez, M. J. Hortigüela, M. L. Ferrer, and F. del Monte, "Highly fluorescent rhodamine B nanoparticles entrapped in hybrid glasses," *Langmuir*, vol. 23, no. 4, pp. 2175–2179, 2007.

[10] A. Lewkowicz, A. Synak, B. Grobelna, L. Kułak, and P. Bojarski, "Spectroscopic properties of rhodamine B entrapped in hybrid porous nanolayers at high dye concentration," *Chemical Physics*, vol. 439, pp. 121–127, 2014.

[11] S. M. And and G. Chumanov, "Light-induced coherent interactions between silver nanoparticles in two-dimensional arrays," *Journal of the American Chemical Society*, vol. 125, no. 10, pp. 2896–2898, 2003.

[12] W. Fang, L. Zhou, B. Shen et al., "Advanced $Bi_2O_{2.7}/Bi_2Ti_2O_7$ composite film with enhanced visible-light-driven activity for the degradation of organic dyes," *Research on Chemical Intermediates*, vol. 44, no. 247, pp. 1–10, 2018.

[13] H. D. L. Secco, F. F. Ferreira, and L. O. Péres, "Simple preparation of fluorescent composite films based on cerium and europium doped LaF_3 nanoparticles," *Journal of Solid State Chemistry*, vol. 259, pp. 43–47, 2018.

[14] K. Aslan, M. Wu, J. R. Lakowicz, and C. D. Geddes, "Fluorescent core–shell $Ag@SiO_2$ nanocomposites for metal-enhanced fluorescence and single nanoparticle sensing platforms," *Journal of the American Chemical Society*, vol. 129, no. 6, pp. 1524-1525, 2007.

[15] M. Lismont, L. Dreesen, B. Heinrichs, and C. A. Páez, "Protoporphyrin IX-functionalized $AgSiO_2$ core–shell nanoparticles: plasmonic enhancement of fluorescence and singlet oxygen production," *Photochemistry and Photobiology*, vol. 92, no. 2, pp. 247–256, 2016.

[16] M. Luoshan, L. Bai, C. Bu et al., "Surface plasmon resonance enhanced multi-shell-modified upconversion $NaYF_4$:Yb^{3+}, Er^{3+} @SiO_2 @Au@TiO_2 crystallites for dye-sensitized solar cells," *Journal of Power Sources*, vol. 307, pp. 468–473, 2016.

[17] Y. Zhang, C. Yang, X. Xiang et al., "Highly effective surface-enhanced fluorescence substrates with roughened 3D flowerlike silver nanostructures fabricated in liquid crystalline phase," *Applied Surface Science*, vol. 401, pp. 297–305, 2017.

[18] R. Ranjan, E. N. Esimbekova, M. A. Kirillova, and V. A. Kratasyuk, "Metal-enhanced luminescence: current trend and future perspectives- a review," *Analytica Chimica Acta*, vol. 971, pp. 1–13, 2017.

[19] M. D. Malinsky, K. L. Kelly, G. C. Schatz, and R. P. van Duyne, "Chain length dependence and sensing capabilities of the localized surface plasmon resonance of silver nanoparticles chemically modified with alkanethiol self-assembled monolayers," *Journal of the American Chemical Society*, vol. 123, no. 7, pp. 1471–1482, 2016.

[20] R. Sun, H. Fu, J. Wang et al., "Surface plasmon enhanced light trapping in metal/silicon nanobowl arrays for thin film photovoltaics," *Journal of Nanomaterials*, vol. 2017, Article ID 4270794, 8 pages, 2017.

[21] R. Wang, R. Sun, H. Fu et al., "Study on preparation of $Ag@SiO_2$ nanoparticles and its optical properties," *Materials Review*, vol. 12, p. 007, 2010.

[22] R. Wang, J. Tang, J. Liu, Y. Wang, and Z. Huang, "Preparation of $Ag@SiO_2$ dispersion in different solvents and investigation of its optical properties," *Journal of Dispersion Science and Technology*, vol. 32, no. 4, pp. 532–537, 2011.

[23] A. Suslov, P. T. Lama, and R. Dorsinville, "Fluorescence enhancement of rhodamine B by monodispersed silver nanoparticles," *Optics Communications*, vol. 345, pp. 116–119, 2015.

[24] Y. Zhang, C. Yang, G. Zhang et al., "Distance-dependent metal enhanced fluorescence by flowerlike silver nanostructures fabricated in liquid crystalline phase," *Optical Materials*, vol. 72, pp. 289–294, 2017.

[25] J. Kümmerlen, A. Leitner, H. Brunner, F. R. Aussenegg, and A. Wokaun, "Enhanced dye fluorescence over silver island films: analysis of the distance dependence," *Molecular Physics*, vol. 80, no. 5, pp. 1031–1046, 1993.

[26] J. R. Lakowicz, "Radiative decay engineering: metal-enhanced fluorescence," in *Principles of Fluorescence Spectroscopy*, pp. 841–859, 2006.

[27] C. D. Geddes and J. R. Lakowicz, "Radiative decay engineering," in *Topics in Fluorescence Spectroscopy*, vol. 8, Springer, Boston, MA, USA, 2005.

[28] I. Gryczynski, J. Malicka, Z. Gryczynski, and J. R. Lakowicz, "Surface plasmon-coupled emission with gold films," *Journal of Physical Chemistry B*, vol. 108, no. 33, pp. 12568–12574, 2004.

[29] J. R. Lakowicz, J. Malicka, I. Gryczynski, and Z. Gryczynski, "Directional surface plasmon-coupled emission: a new method for high sensitivity detection," *Biochemical and Biophysical Research Communications*, vol. 307, no. 3, pp. 435–439, 2003.

[30] K. Aslan, Z. Leonenko, J. R. Lakowicz, and C. D. Geddes, "Annealed silver-island films for applications in metal-enhanced fluorescence: interpretation in terms of radiating plasmons," *Journal of Fluorescence*, vol. 15, no. 5, pp. 643–654, 2005.

[31] W. L. Barnes, "Fluorescence near interfaces: the role of photonic mode density," *Journal of Modern Optics*, vol. 45, no. 4, pp. 661–699, 1998.

[32] P. J. Tarcha, J. Desaja-Gonzalez, S. Rodriguez-Llorente, and R. Aroca, "Surface-enhanced fluorescence on SiO_2-coated silver island films," *Applied Spectroscopy*, vol. 53, no. 1, pp. 43–48, 1999.

[33] C. J. Murphy, T. K. Sau, C. J. Orendorff, and A. M. Gole, *Surface Enhanced Raman Spectroscopy Using Shaped Gold Nanoparticles*, WO, 2012.

[34] C. J. Stephenson, "Fluorescent probes and switches based on the xanthene dyes rhodamine and fluorescein," vol. 240, Acs National Meeting Book of Abstracts, Washington, D.C., USA, 2010.

[35] Y. X. Liu and Q. Z. Zhai, "Preparation, characterization and optical properties of MCM-41/rhodamine B," *Bulletin of the Chemical Society of Ethiopia*, vol. 23, no. 1, pp. 145–150, 2009.

[36] Y. Oba and S. R. Poulson, "Octanol-water partition coefficients (K_{ow}) vs. pH for fluorescent dye tracers (fluorescein, eosin Y), and implications for hydrologic tracer tests," *Geochemical Journal*, vol. 46, no. 6, pp. 517–520, 2013.

[37] Y. Li, C. Xie, S. Peng, G. Lu, and S. Li, "Eosin Y-sensitized nitrogen-doped TiO_2 for efficient visible light photocatalytic hydrogen evolution," *Journal of Molecular Catalysis A Chemical*, vol. 282, no. 1-2, pp. 117–123, 2008.

[38] A. Synak, B. Grobelna, S. Raut et al., "Metal enhanced fluorescence of flavin mononucleotide using new plasmonic platform," *Optical Materials*, vol. 59, pp. 136–140, 2016.

[39] F. Cannone, G. Chirico, A. R. Bizzarri, and S. Cannistraro, "Quenching and blinking of fluorescence of a single dye molecule bound to gold nanoparticles," *The Journal of Physical Chemistry B*, vol. 110, no. 33, pp. 16491–16498, 2006.